

# WMO statement on the status of the global climate in 2013



**World  
Meteorological  
Organization**

Weather · Climate · Water

WMO-No. 1130

WMO-No. 1130

© **World Meteorological Organization, 2014**

The right of publication in print, electronic and any other form and in any language is reserved by WMO. Short extracts from WMO publications may be reproduced without authorization, provided that the complete source is clearly indicated. Editorial correspondence and requests to publish, reproduce or translate this publication in part or in whole should be addressed to:

Chair, Publications Board  
World Meteorological Organization (WMO)  
7 bis, avenue de la Paix  
P.O. Box 2300  
CH-1211 Geneva 2, Switzerland

Tel.: +41 (0) 22 730 84 03  
Fax: +41 (0) 22 730 80 40  
E-mail: [Publications@wmo.int](mailto:Publications@wmo.int)

ISBN 978-92-63-11130-2

WMO, in collaboration with Members, began issuing annual statements on the status of the global climate in 1993. This publication was issued in collaboration with the Hadley Centre of the UK Meteorological Office, United Kingdom of Great Britain and Northern Ireland; the Climatic Research Unit (CRU), University of East Anglia, United Kingdom; the Climate Prediction Center (CPC), the National Climatic Data Center (NCDC), the National Environmental Satellite, Data, and Information Service (NESDIS), the National Hurricane Center (NHC) and the National Weather Service (NWS) of the National Oceanic and Atmospheric Administration (NOAA), United States of America; the Goddard Institute for Space Studies (GISS) operated by the National Aeronautics and Space Administration (NASA), United States; the Japan Meteorological Agency (JMA), Japan; the European Centre for Medium-Range Weather Forecasts (ECMWF), United Kingdom; the Global Precipitation Climatology Centre (GPCC), Germany; the Global Snow Laboratory, Rutgers University, United States; the National Snow and Ice Data Center (NSIDC), United States; the Colorado Center for Astrodynamic Research, University of Colorado-Boulder, United States; the Polar Science Center, University of Washington, United States; the Commonwealth Scientific and Industrial Research Organization (CSIRO) Marine and Atmospheric Research, Australia; and the Vienna University of Technology, Austria. Other contributors are the National Meteorological and Hydrological Services or equivalent climate institutions of Argentina, Armenia, Australia, Belarus, Bosnia and Herzegovina, Brazil, Bulgaria, Canada, China, Cyprus, Czech Republic, Denmark, Estonia, Fiji, Finland, France, Germany, Guinea, Hungary, Iceland, India, Iran (Islamic Republic of), Ireland, Israel, Japan, Jordan, Kenya, Latvia, Lithuania, Luxembourg, Malta, Mexico, Montenegro, Morocco, Nigeria, Norway, Pakistan, Portugal, Republic of Moldova, Romania, Russian Federation, Serbia, Slovakia, Slovenia, South Africa, Spain, Sweden, Switzerland, Thailand, Tunisia, Turkey, Ukraine, United Kingdom, United Republic of Tanzania and United States. The WMO Regional Association VI (Europe) Regional Climate Centre on Climate Monitoring, the African Centre of Meteorological Applications for Development (ACMAD, Niamey), the Hong Kong Observatory (HKO), Hong Kong, China, the Australian Research Council (ARC) Centre of Excellence for Climate System Science, University of Melbourne, Australia, and the International Research Centre on El Niño (CIIFEN, Guayaquil, Ecuador) also contributed.

Cover illustration: Praveen Agrawal / WFP

#### NOTE

The designations employed in WMO publications and the presentation of material in this publication do not imply the expression of any opinion whatsoever on the part of WMO concerning the legal status of any country, territory, city or area, or of its authorities, or concerning the delimitation of its frontiers or boundaries.

The mention of specific companies or products does not imply that they are endorsed or recommended by WMO in preference to others of a similar nature which are not mentioned or advertised.

The findings, interpretations and conclusions expressed in WMO publications with named authors are those of the authors alone and do not necessarily reflect those of WMO or its Members.

# Contents

<b>Foreword</b> . . . . .	<b>2</b>
<b>Preface</b> . . . . .	<b>3</b>
<b>Key findings</b> . . . . .	<b>4</b>
Temperatures . . . . .	4
Rain, snow and ice . . . . .	5
Oceans . . . . .	7
Regional highlights . . . . .	8
Tropical cyclones . . . . .	15
Greenhouse gases and ozone-depleting substances . . . . .	17
<b>Major weather and climate events around the world in 2013</b> . . . . .	<b>19</b>
<b>Explaining the summer 2012/2013 and annual 2013 record warmth in Australia</b> . . . . .	<b>20</b>

# Foreword


The dramatic impact of climate variability and climate change continued to be felt all over the world throughout 2013. The *WMO Statement on the Status of the Global Climate in 2013* provides a snapshot of global and regional trends in weather and climate over the past year and highlights some of the year's most significant extreme events.

The year 2013 tied with 2007 as the sixth warmest since global records began in 1850. Although the climate varies naturally from year to year, it is clear that the planet is experiencing an overall warming trend. Thirteen of the fourteen warmest years on record have all occurred in the twenty-first century, and each of the past three decades has been warmer than the last, culminating with 2001–2010 as the warmest decade on record. As highlighted by the Fifth Assessment Report of the Intergovernmental Panel on Climate Change, this steady warming is caused by rising levels of anthropogenic greenhouse gases in the atmosphere.

We now have a better understanding of human-induced climate change, and climate scientists can increasingly determine how large-scale pressure and temperature patterns influence the weather. The best known of these is the El Niño-Southern Oscillation (ENSO) in the Pacific Ocean, which affects weather patterns around the world through "teleconnections". In addition to ENSO, the North Atlantic Oscillation, the Arctic Oscillation, jet streams and other recurring patterns also often explain why weather conditions are wetter, drier, warmer, cooler or stormier than average.

Weather forecasting, including the prediction of storms and other hazards, has greatly evolved in recent years. In October 2013, the events surrounding Cyclone *Phailin*, the second strongest tropical cyclone to strike India since modern records began, showed how improved forecasting, combined with government action to build national resilience and provide shelters, greatly reduces the loss of life. Nevertheless, extreme events can still cause fatalities and destroy property, so we must continue enhancing preparedness, strengthening early warning systems and implementing a multi-hazard approach to disaster risk reduction.

The Statement draws on input from leading research institutions and from the National Meteorological and Hydrological Services of WMO Members. This summary has been published in all six official WMO languages in order to reach the broadest possible readership. However, I also strongly encourage interested readers to examine the more detailed underlying report, which is available on the WMO website.



(M. Jarraud)  
Secretary-General

# Preface

This Statement is based on datasets and information that were made available by WMO Members and partners for 2013 and assessed in their global and regional geographical context. Comparisons were made with climatological averages and records (historical background) whenever possible and appropriate.

The global temperature assessment is based on three independent datasets that are maintained by the Met Office Hadley Centre and the Climatic Research Unit of the University of East Anglia (HadCRU), both in the United Kingdom; the National Climatic Data Center of the National Oceanic and Atmospheric Administration (NCDC–NOAA), based in the United States; and the Goddard Institute for Space Studies (GISS) operated by the National Aeronautics and Space Administration (NASA), also in the United States. The HadCRU dataset extends back to 1850, and the NCDC and GISS datasets (and hence the combined dataset) extend back to 1880. Other datasets have also been used for additional analysis.

The content was developed and peer-reviewed by several experts affiliated with international and regional climate institutions, centres and programmes, and by the world's National Meteorological and Hydrological Services (NMHSs), the main providers of the underlying observations and climate information. More than 50 NMHSs provided direct input

to the Statement following the WMO call for contributions. Many others made their data and climate reports available on their websites, and these were accessed when necessary. When doubts arose as to facts and figures, WMO communicated with the relevant national source in order to verify the information before its inclusion in the Statement. The definition of the Regions is based on the WMO regional structure, as follows:

- Africa (Region I)
- Asia (Region II)
- South America (Region III)
- North America, Central America and the Caribbean (Region IV)
- South-West Pacific (Region V)
- Europe (Region VI)

WMO Climate System Monitoring uses Essential Climate Variables (ECVs) as defined by the Global Climate Observing System. Some 50 ECVs have been identified as fundamental for global observation. This Statement incorporates assessments of the status of the global climate and observed extremes detected using ECV data and products, including air temperature, precipitation, stratospheric ozone and long-lived greenhouse gases (atmospheric ECVs); snow cover, ice sheets and soil moisture (terrestrial ECVs); as well as sea ice, sea level rise, sea surface temperature and ocean acidification (oceanographic ECVs).

# Key findings

Figure 1. Global land air surface and sea surface temperature anomalies (°C) for 2013, relative to 1961–1990  
(Source: Met Office Hadley Centre, United Kingdom, and Climatic Research Unit, University of East Anglia, United Kingdom)

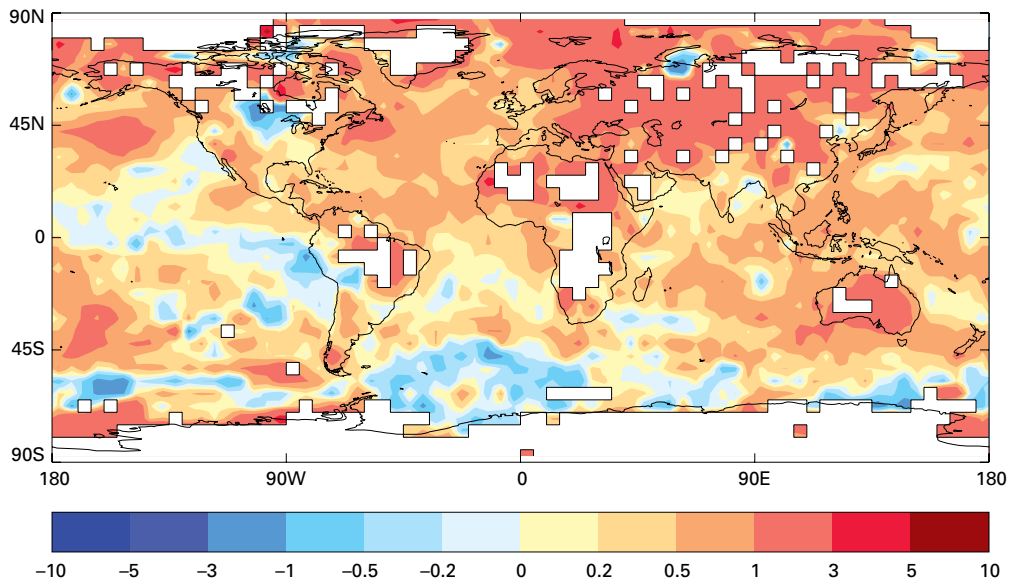


Figure 2. Annual global average temperature anomalies (relative to 1961–1990) from 1850 to 2013 from the Hadley Centre/CRU (HadCRUT4) (black line and grey area, representing average and 95 per cent uncertainty range), the NOAA National Climatic Data Center (red), and the NASA Goddard Institute for Space Studies (blue)  
(Source: Met Office Hadley Centre, United Kingdom, and Climatic Research Unit, University of East Anglia, United Kingdom)

## TEMPERATURES

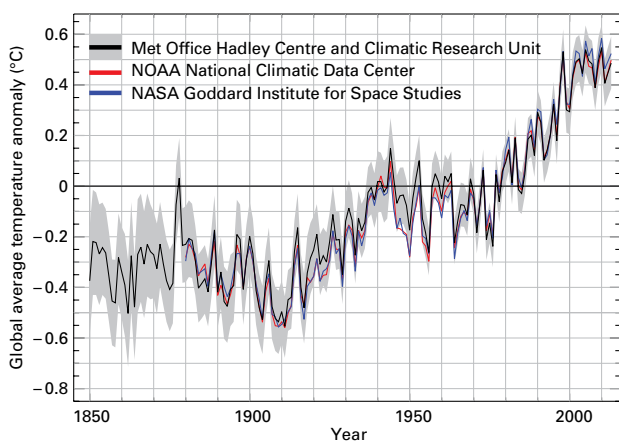
The year 2013 tied with 2007 as the sixth warmest since global records began in 1850. The global average surface temperature was  $0.50^{\circ}\text{C} \pm 0.10^{\circ}\text{C}$  ( $0.90^{\circ}\text{F} \pm 0.18^{\circ}\text{F}$ ) above the 1961–1990 average and  $0.03^{\circ}\text{C}$  ( $0.05^{\circ}\text{F}$ ) above the 2001–2010 average. The past year was also warmer than both 2011 and 2012, which, though marked by cooling La Niña conditions, were  $0.43^{\circ}\text{C}$  and  $0.46^{\circ}\text{C}$  above average, respectively.

Warming El Niño and cooling La Niña events are major drivers of natural variability in the climate system. Neither condition was present during 2013, which was among the four warmest

ENSO-neutral years on record. Thirteen of the fourteen warmest years on record, including 2013, have all occurred in the twenty-first century. The warmest on record are 2010 and 2005, followed by 1998. El Niño conditions dominated the early months of 2010 and 1998, and weak El Niño-type conditions extended from 2004 to the first half of 2005.

To arrive at these figures, WMO takes an average of the three main global temperature datasets, which are managed separately and use different methodologies. Other datasets produce similar but slightly different results. A separate temperature analysis conducted by the Japan Meteorological Agency, for example, estimates that 2013 was the second warmest year on record. According to reanalysis data from the European Centre for Medium-Range Weather Forecasts, 2013 tied with 1998 as the fourth warmest since 1958.

Because the capacity for heat absorption differs over land and over sea, the air over the land tends to warm up faster. Across the world's land surfaces, the 2013 global air temperature was  $0.85^{\circ}\text{C} \pm 0.17^{\circ}\text{C}$  above the 1961–1990 average and  $0.06^{\circ}\text{C}$  above the 2001–2010 average, the fourth highest on record. A very warm November–December period that ranked second behind 2006 contributed to this high temperature anomaly. Over the global ocean, the surface temperature for 2013 tied with 2004 and 2006 as



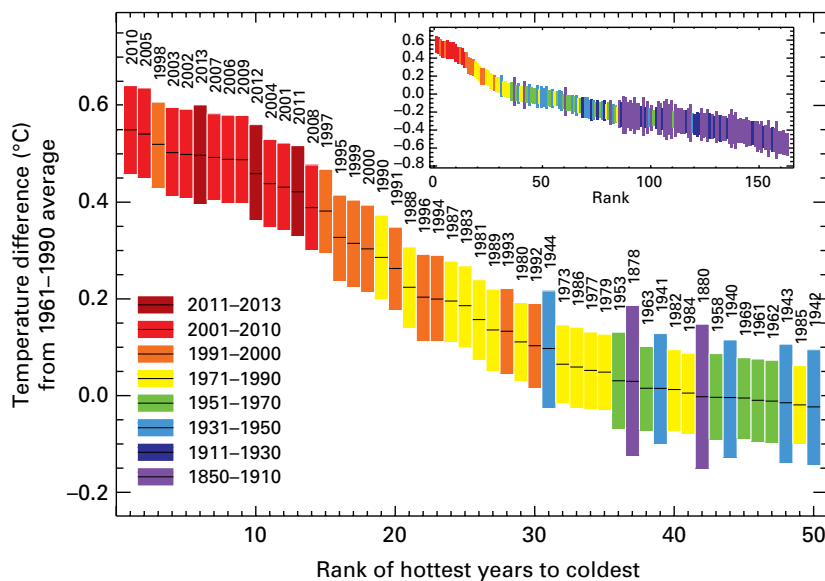
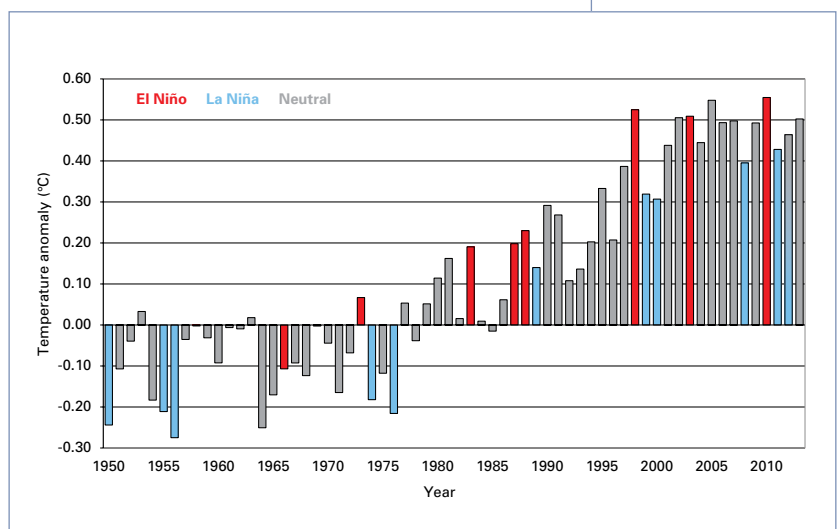


Figure 3. Global ranked land and ocean surface temperatures for the warmest 50 years. Inset shows global ranked surface temperatures from 1850. The size of the bars indicates the 95 per cent confidence limits associated with each year. Values are simple area-weighted averages for the whole year. (Source: Met Office Hadley Centre, United Kingdom, and Climatic Research Unit, University of East Anglia, United Kingdom)

the sixth warmest on record, at  $0.35^{\circ}\text{C} \pm 0.07^{\circ}\text{C}$  above the 1961–1990 average.

The northern hemisphere’s weather patterns during early 2013 were largely influenced by the Arctic Oscillation. This brought cooler-than-average spring temperatures to much of Europe, the south-eastern United States, north-western Russian Federation and parts of Japan. The Arctic region, meanwhile, was considerably warmer than average, along with much of central and northern Africa, the eastern Mediterranean, southern Russian Federation and much of China. This so-called warm Arctic, cold continents pattern is characteristic of the Arctic Oscillation’s negative phase. The year 2013 saw the most negative Arctic Oscillation on record for the month of March. A similar pattern with high pressure over Greenland and low pressure to the south re-emerged in late spring, once again causing cold Arctic air to surge into western and central Europe.

In the southern hemisphere, summer was extremely warm, with monthly January temperature anomalies reaching  $+5^{\circ}\text{C}$  in parts of Australia. Exceptional warm conditions were also present during the winter, with New Zealand experiencing its warmest winter on record. The beginning of austral summer 2013/2014 was very hot in parts of South America, with the December temperature reaching new record highs. As a result of the continued warmth



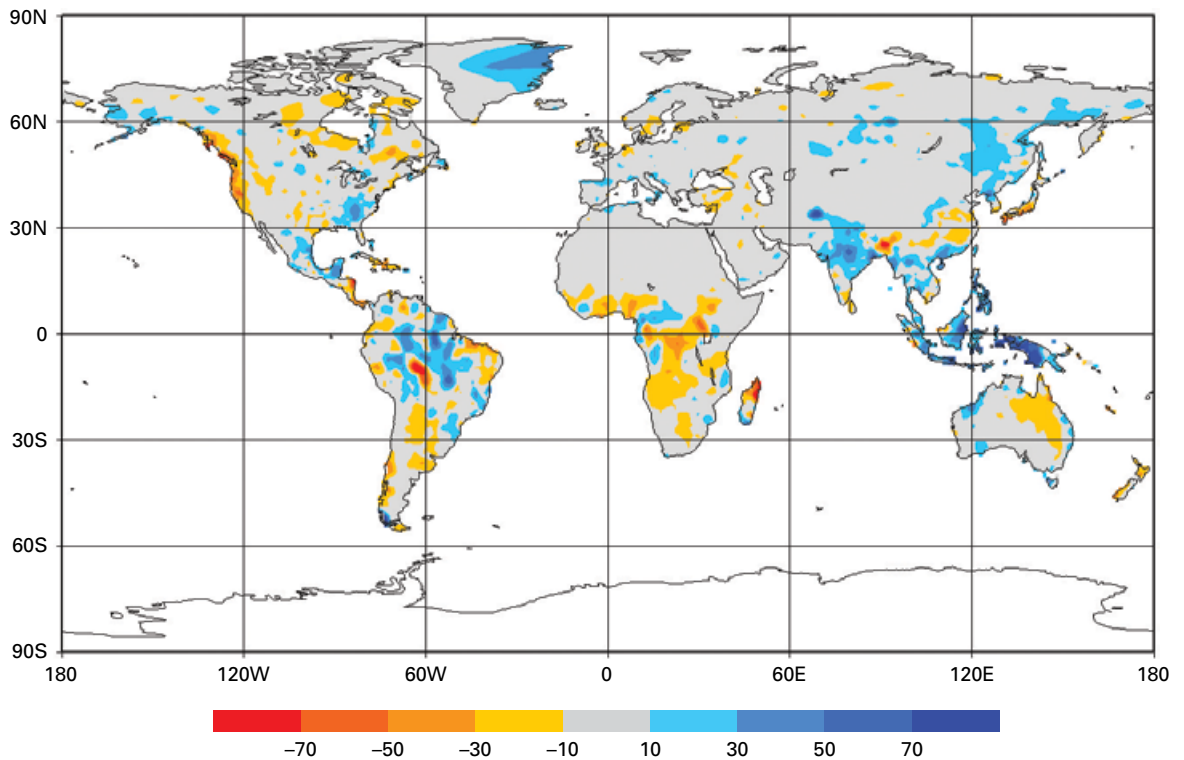
throughout the year across parts of the southern hemisphere, 2013 was the warmest year on record in Australia, second warmest in Argentina and third warmest in New Zealand. Modelling experiments have indicated that the odds of the record Australian hot summer occurring were increased fivefold by human-induced climate change (see page 20 and accompanying figure).

## RAIN, SNOW AND ICE

Global precipitation during 2013 equalled the 1961–1990 average of 1 033 mm, according to the National Oceanic and Atmospheric Administration (United States). Precipitation at

Figure 4. January–December global land and ocean surface temperature anomalies (relative to 1961–1990) for the period 1950–2013; years that started with a moderate or strong La Niña already in place are shown in blue; years that started with a moderate or strong El Niño already in place are shown in red; other years are shown in grey.

Figure 5. Annual precipitation anomalies for global land areas for 2013; gridded 1.0-degree raingauge-based in mm/month (relative to 1951–2000) (Source: Global Precipitation Climatology Centre, Deutscher Wetterdienst, Germany)



the regional level, however, varied significantly. For example, wetter-than-average conditions were seen across most of Greenland, the southern Arabian Peninsula, central India and western China. Drier-than-average conditions were present over the western United States, much of northern Canada, northern Siberia and the eastern inland of Australia.

Winter snow cover in North America has varied widely over the past few years. During the 2012/2013 winter, snow cover extent was 500 000 km<sup>2</sup> above the 1981–2010 average, resulting in the fourteenth largest winter extent for the continent since records began in 1966. During the spring, North American snow cover was 830 000 km<sup>2</sup> above average, making it the tenth largest spring extent for the continent and the largest since 1997.

During the same period, snow cover extent across the Eurasian continent was 1.71 million km<sup>2</sup> above the 1981–2010 average, the third largest winter extent on record for this region and the largest since 2003. In the spring, the continent's snow cover contracted significantly to 430 000 km<sup>2</sup> below average, resulting in the fourteenth smallest extent on record for the season. In May,

Eurasian snow cover dipped to 7.3 million km<sup>2</sup>, setting a new record low for that month.

As further evidence of the rapid response of the Arctic cryosphere to increasing air temperatures, the northern hemisphere June snow cover is currently decreasing at a faster rate than Arctic summer minimum sea-ice extent, and at rates that exceed the projection of climate models. June 2013 snow cover across the hemisphere was the second lowest, greater only than the record low of 2012.

Soil moisture is a key variable for monitoring the climate system because it strongly influences the exchange of water and energy between the land surface and the atmosphere. Very wet soil conditions resulting from hydrometeorological events were noticeable and had an impact on floods in a number of regions including eastern parts of the Russian Federation, north-eastern China, India, the Philippines and central Europe. On the other hand, annual soil moisture anomalies indicated dryness in the southern hemisphere, where Australia, South America and southern Africa experienced severe drought conditions during the first part of the year.



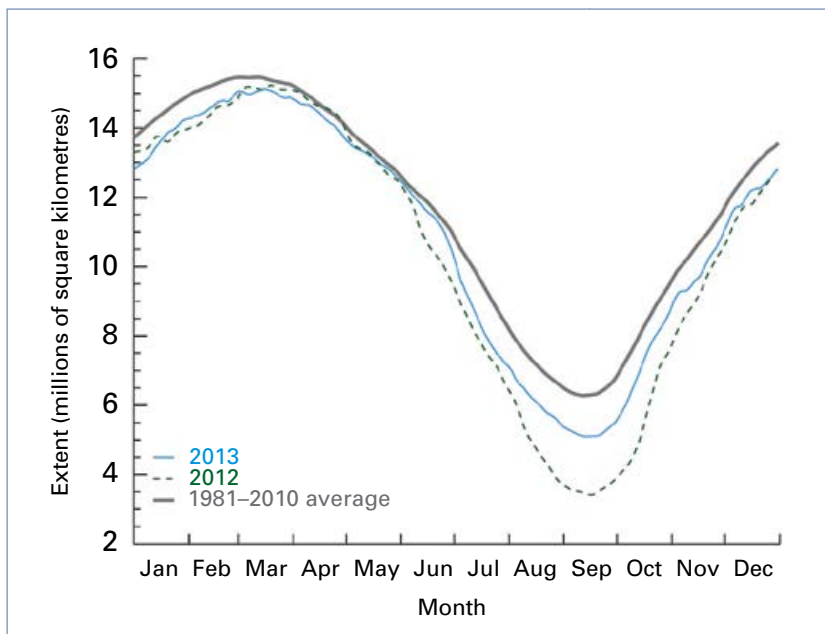
Arctic sea-ice extent reached its annual maximum on 15 March at 15.13 million km<sup>2</sup>. This was approximately 0.5 million km<sup>2</sup> below the average 1981–2010 annual maximum, making it the sixth smallest maximum sea-ice extent since satellite records began in 1979. During the 2012/2013 growth season, Arctic sea-ice extent grew by 11.72 million km<sup>2</sup>, the largest seasonal increase on record; this growth can be explained by the record small sea-ice extent of September 2012. Arctic maximum sea-ice extent in March has decreased at an average rate of 2.6 per cent per decade.

Another way to assess the state of the Arctic sea ice is to estimate the age of the ice, given that first-year ice is the thinnest and most susceptible to melting. Ice that was four years of age and older decreased from 18 per cent of the ice cover in March 1984 to 2 per cent in March 2012. It increased slightly to 3 per cent in 2013. In March 1984, 56 per cent of the ice pack was composed of first-year ice, while in March 2013 first-year ice comprised 78 per cent of total ice cover at its peak.

The Arctic reached its annual minimum sea-ice cover on 13 September, at 5.10 million km<sup>2</sup> or 18 per cent below the 1981–2010 average minimum, making it the sixth smallest annual minimum on record. All seven of the lowest Arctic sea-ice extents in the satellite record have occurred in the last seven years, beginning with 2007. September Arctic sea-ice extent has decreased at an average rate of 13.7 per cent per decade. The total minimum sea-ice volume, which combines measures of ice extent and model simulations of ice thickness, was higher in 2013 than in 2010, 2011 and 2012, but lower than in 2007 and well below the 1979–2012 average.

February marked the end of the Antarctic sea-ice melt season in 2013. The annual minimum extent of sea ice was reached on 20 February at 3.68 million km<sup>2</sup>. This was the second largest annual minimum sea-ice extent for Antarctica. In addition, Antarctic sea-ice extent reached a record maximum for the second year in a row. On 1 October, it was 19.57 million km<sup>2</sup>, 2.7 per cent higher than the 1981–2010 average.

September Antarctic sea-ice extent has increased at an average rate of 1.1 per cent per decade.



Scientists believe that changes in atmospheric circulation over the past three decades, which have weakened the prevailing winds that circle Antarctica, may be a factor. The increasing extent of the ice may also be linked to changing ocean circulation and a build-up of cold freshwater on the surface of the Southern Ocean due to increasing precipitation and melting land-based ice shelves.

Melting at the surface of the Greenland ice sheet was much less dramatic in 2013 than in the record year of 2012. It peaked in late July, when satellites detected melting over 44 per cent of the surface. This coincided with record warmth in south-western Greenland (30 July saw a temperature of 25.9°C in Maniitsoq, the highest temperature ever recorded in Greenland). The last decade has experienced accelerated melting of the sea-ice cover and mass loss of the Greenland ice sheet.

## OCEANS

The ocean acts as an effective buffer for the climate system by absorbing and storing a large amount of excess carbon and heat from the atmosphere. It has absorbed approximately one quarter of all the carbon dioxide (CO<sub>2</sub>) released into the atmosphere by humans since the start of the industrial revolution. This absorbed CO<sub>2</sub> forms a weak carbonic acid, which causes ocean

Figure 6. Arctic sea-ice extent in 2013, compared with 2012 and the 1981–2010 average (Source: National Snow and Ice Data Center, United States)

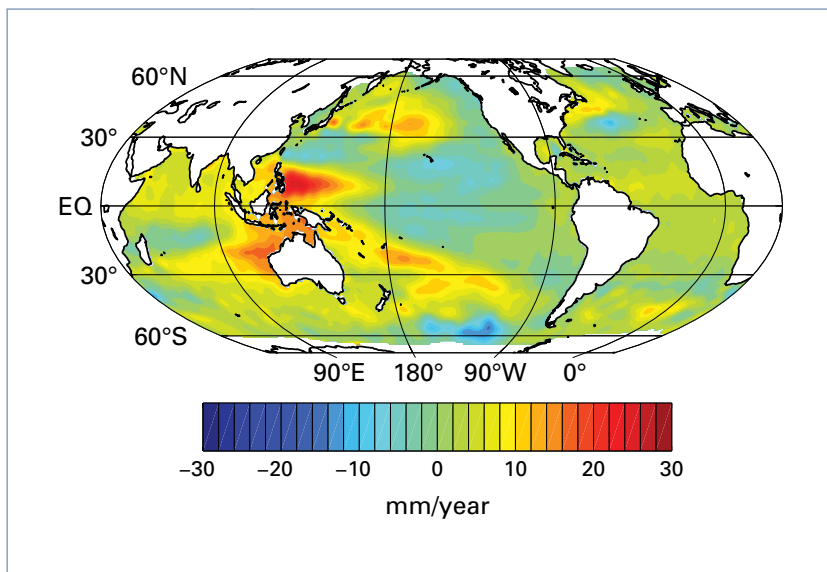


Figure 7. Sea level trends for the period 2003–2013 (Source: Commonwealth Scientific and Industrial Research Organization (CSIRO) Marine and Atmospheric Research, Australia)

acidification. As a result, the pH of the ocean has decreased by 0.11, which corresponds approximately to a 30 per cent increase in acidity. Ocean acidification is already harming corals, shellfish and other marine life.

While the rate at which surface air temperatures are rising has slowed in recent years, heat continues to be trapped in the Earth system, mostly as increased ocean heat content. About 93 per cent of the excess heat trapped in the Earth system between 1971 and 2010 was taken up by the ocean. From around 1980 to 2000, the ocean gained about 50 zettajoules ( $10^{21}$  joules) of heat. Between 2000 and 2013, it added about three times that amount. Prior to 2000, most of the heat was trapped between the sea surface and a depth of 700 m. Since then, most of the heat has been stored at depths of 700 m to 2 000 m. The increased uptake in this region may be due to changes in atmospheric and ocean circulation patterns in the tropical Pacific and to interactions with large-scale climate patterns such as ENSO and the Pacific Decadal Oscillation.

Globally, sea level has risen by 19 cm since the start of the twentieth century, mostly because of the thermal expansion of the oceans and the melting of glaciers and ice caps. Since measurements began in 1993, sea level has been rising at about 2.9–3.2 mm/yr (based on two separate estimates, each with an uncertainty of  $\pm 0.4$  mm/yr), with some year-to-year variability.

This range encompasses the observed rate of about 3 mm/yr for the 2001–2010 decade and is around double the observed twentieth century trend of 1.6 mm/yr.

Preliminary analyses indicate that the global average sea level reached a new record high in March. Some regions of the globe are experiencing greater sea-level rise than others (some are even experiencing declining sea levels) due to local variations in currents, land movements and ocean warming. The region of the Pacific Ocean near the Philippines has observed some of the highest rising sea-level rates over the past half century. This contributed to the enormous devastation in parts of the Philippine islands, when Typhoon *Haiyan* struck in November and caused a massive storm surge.

## REGIONAL HIGHLIGHTS

### AFRICA

The continent experienced an overall hot year, with 2013 ranking as the second warmest on record, behind 2010. The temperature in Violsdrif, South Africa, soared to 47.3°C on 4 March – the hottest March temperature ever measured in Africa. In West Africa, the temperature in Navrongo, Ghana, reached 43°C on 6 March, the warmest temperature ever measured in Ghana. Several temperature records were also broken in Kenya. Spring and October temperatures in Tunisia, which were



Women collect water at the Chaquelane resettlement camp near the flood hit town of Chokwe, in southern Mozambique.

AGNIESZKA FLAK/REUTERS

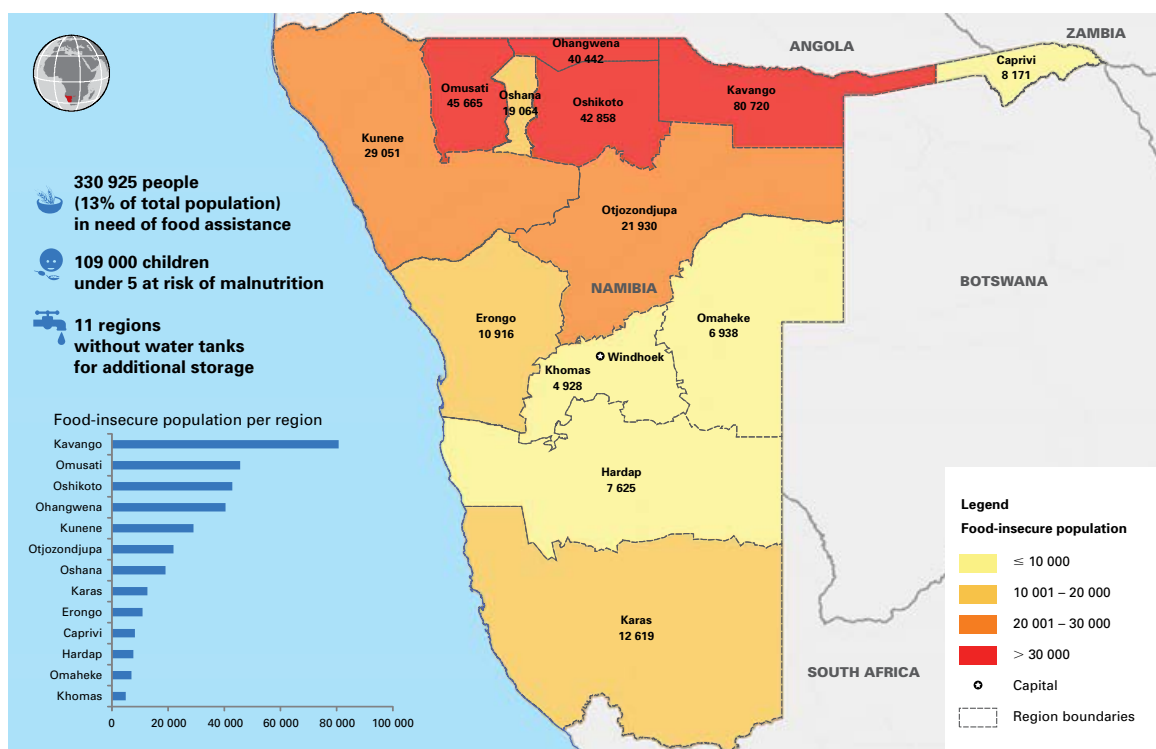


Figure 8. Map indicating the number of people facing food insecurity in Namibia in May 2013 due to ongoing drought conditions (Source: United Nations Office for the Coordination of Humanitarian Affairs)

2.2°C and 4°C above average, respectively, contributed to one of the 10 warmest years in the country since 1950.

Above-average precipitation occurred in northern Mali and adjacent areas in Algeria. Below-average precipitation was recorded along the Gulf of Guinea, from Côte d'Ivoire to Nigeria and over the southernmost parts of Ghana, Benin and Togo.

Following nearly three decades of low seasonal rainfall and a second consecutive year of failed rains, Angola and Namibia suffered one of the worst droughts of the past 30 years. An estimated 1.5 million people in southern Angola faced food insecurity, as did nearly 800 000 in Namibia. Historic drought conditions also affected La Réunion from May to September.

In Mozambique, severe flooding that killed at least 113 people and displaced 185 000 occurred in January. Heavy rainfall between March and April led to flooding that damaged crops and displaced thousands of people throughout parts of southern Somalia and eastern Kenya. Heavy rains also fell in Sudan in August, causing

severe damage, killing 76 people and affecting some 500 000. Bamako, Mali, and Marrakech, Morocco were also affected by floods.

## ASIA

Summer was extremely hot in many parts of Asia. Japan, for example, had its hottest summer on record, including a national record high of 41°C in Shimanto, Kochi Prefecture, on 12 August. Many daily maximum temperature records were broken in Hong Kong, China, in March and April, with some locations exceeding 40°C.

China saw its fourth warmest year since national records began in 1961. The most severe heat-wave since 1951 occurred in southern China between July and August, with temperatures over 40°C. The region also experienced severe drought conditions. Approximately 78 million people and over 8 million hectares of farmland were affected, with direct economic losses estimated at US\$ 7.7 billion.

In India, Nagpur recorded its all-time high temperature of 47.9°C on 22 May, while Amritsar observed its highest ever temperature of 48°C

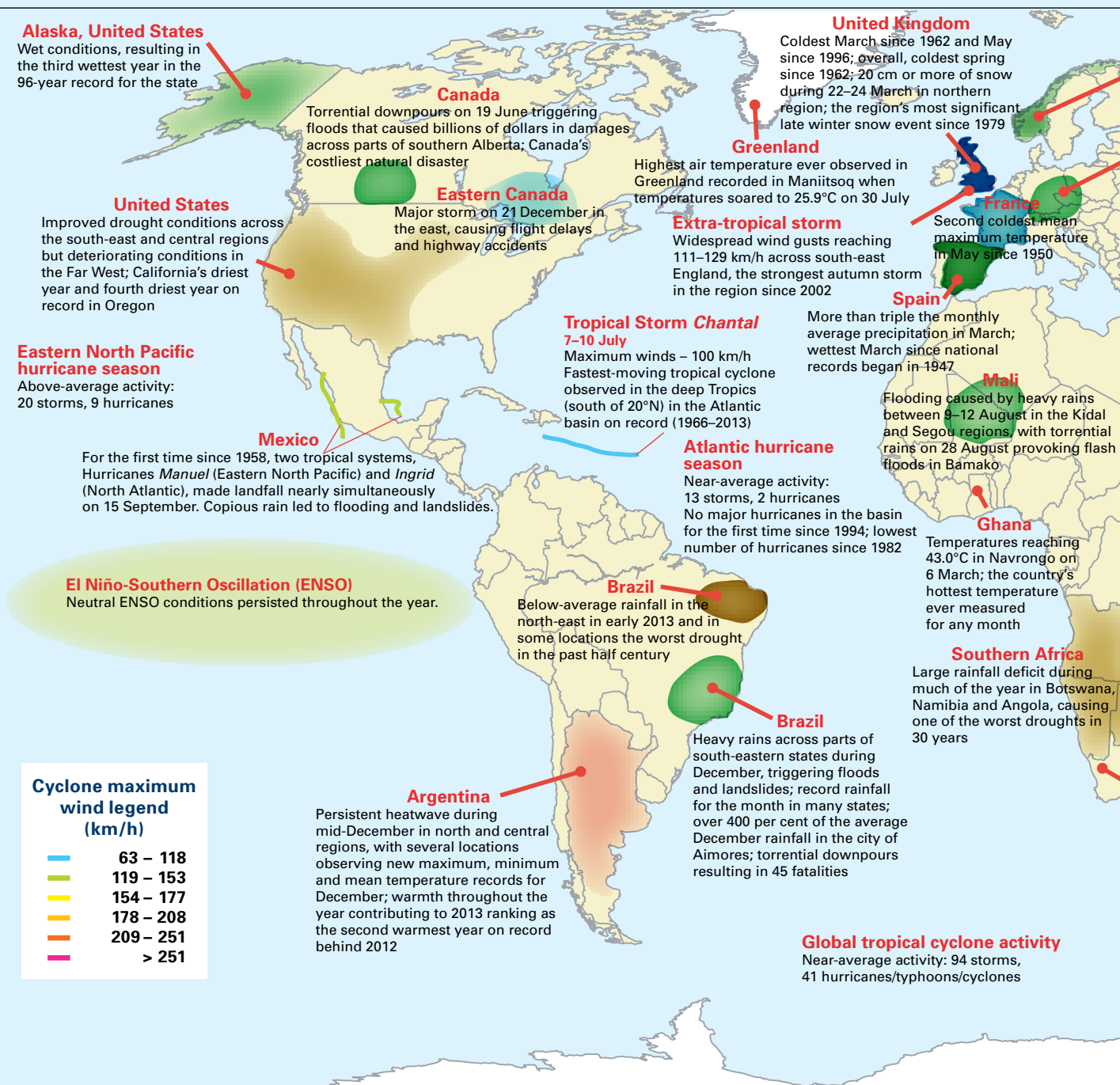
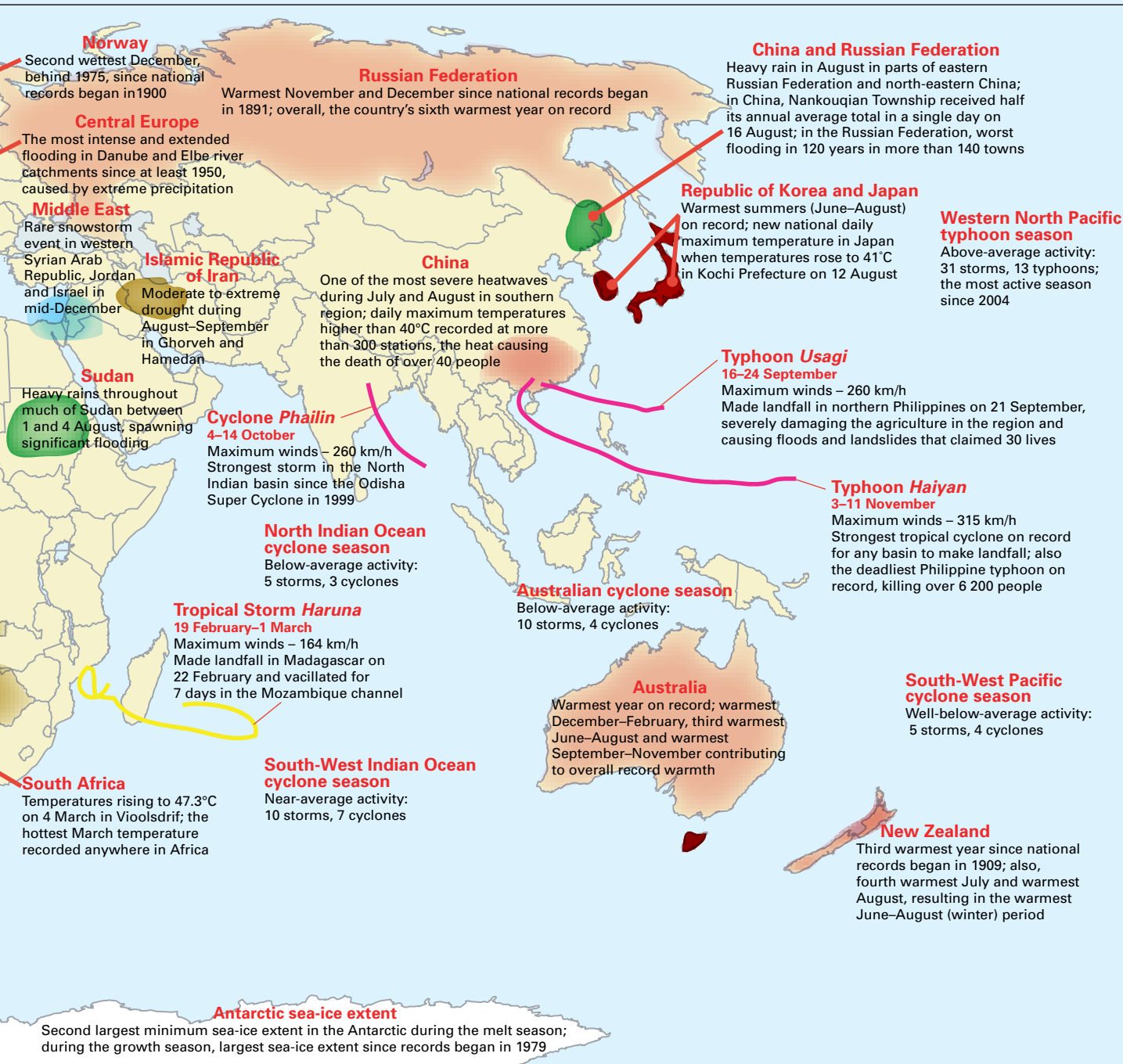


Figure 9. Significant climate anomalies and events in 2013  
(Source: National Climatic Data Center, NOAA, United States)



## TROPICAL CYCLONE CATEGORY

Hurricane, cyclone and typhoon are different terms for the same weather phenomenon that is accompanied by torrential rain and maximum sustained wind speeds (near centre) exceeding 119 kilometres per hour. Such a weather phenomenon is referred to by the following name depending on the region:

- Hurricane: Western North Atlantic, central and eastern North Pacific, Caribbean Sea and Gulf of Mexico;
- Typhoon: Western North Pacific;
- Cyclone: Bay of Bengal and Arabian Sea;
- Severe tropical cyclone: Western South Pacific and South-East Indian Ocean;
- Tropical cyclone: South-West Indian Ocean.



A boy jumps into a water canal to cool himself with others on a hot day in the eastern city of Lahore, Pakistan.

on both 23 and 24 May. More than 2 700 people perished due to the heat. South-west Asian monsoon rainfall for the country as a whole was 106 per cent of the average, but was characterized by regional variations. The monsoon had an early onset over all of India and brought the worst flooding and devastation in the past half century to regions near the India-Nepal border. North-western India received nearly double its average June rainfall; thousands of people were killed and many more went missing.

Pakistan saw its most severe heatwave in decades, with temperatures reaching 51°C in Larkana, the highest May temperature in the city since 1998. Cotton crops and rice paddies were damaged, and more than 100 people died. Punjab and Sindh provinces were inundated by floods due to heavy monsoon rains during most of August. The floods covered about 200 000 km<sup>2</sup>, killing an estimated 250 people and affecting nearly 1.5 million.

Northern East Asia had a cold period during its 2012/2013 winter season, associated with negative Arctic Oscillation conditions and blocking patterns around eastern Siberia. Most of Siberia was 2°C–3°C below average, making this one of its coldest winters of the twenty-first century.

From the end of July to mid-August, unusually heavy rain fell near the Amur river, which marks the border between China and the Russian

Federation. The Songhuajiang and Liaohe river basins in north-eastern China saw their heaviest floods since 1998. Massive flooding was also reported in eastern Russian Federation. More than 140 towns were affected by the worst flooding in 120 years.

## SOUTH AMERICA

Temperatures in South America were dominated by hot conditions in most parts of the continent, except for some limited areas in southern Brazil and the north-central and western parts of South America, which had near to colder than average temperatures. A warm October–December period – including the hottest December on record – contributed to the second warmest year in Argentina since records began in 1961, behind only the record warmth of 2012. In December, the most significant heatwave since 1987 struck central and northern Argentina.

North-eastern Brazil experienced its worst drought in 50 years. This followed the 2001–2010 decade, when large parts of the Amazon Basin saw prolonged drought. The Brazilian Plateau, which is the core monsoon region in South

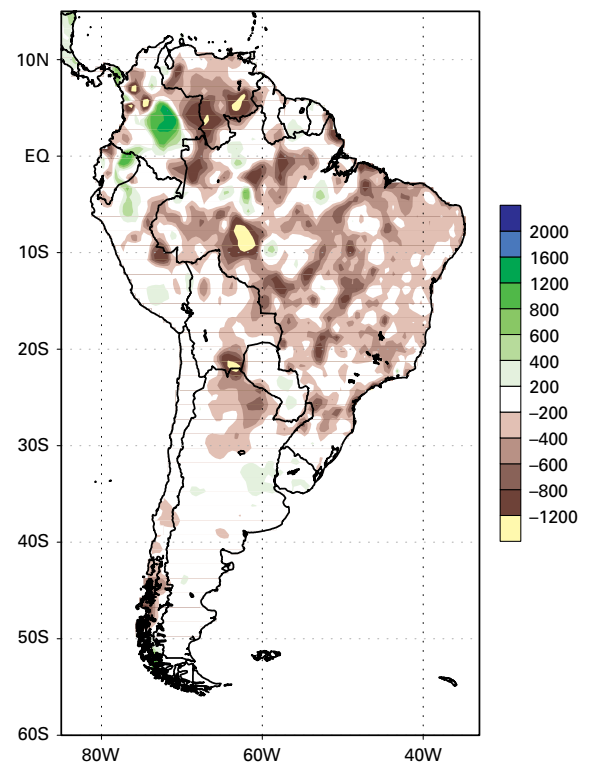


Figure 10. Precipitation anomalies over South America during the active monsoon season, September 2012–May 2013  
(Sources: NOAA Climate Prediction Center, United States, and Instituto Nacional de Meteorologia and Centro de Previsão de Tempo e Estudos Climáticos, Brazil)

America, experienced its largest rainfall deficit since records began in 1979; damages exceeded US\$ 8 billion.

On 2 April, La Plata, Argentina, received about 300 mm of rainfall in just three hours. The torrential downpour led to flash floods that resulted in more than 50 fatalities, making this one of the worst weather disasters in the history of Argentina. Many states in Brazil also had extremely heavy rainfall during December, with at least seven cities setting new precipitation records. In south-eastern Brazil, the city of Aimores received more than four times its average rainfall for the month.

### NORTH AMERICA, CENTRAL AMERICA AND THE CARIBBEAN

Temperatures across most of North America were above average during 2013, but were more moderate overall than in 2012. Winter was warmer than average in Canada and the United States, although spring in the contiguous United States was the coolest since 1996. Temperatures in the United States rebounded during the summer, and the warmth continued into September.

Summer in Alaska was the second hottest on record, and October–December was the sixth warmest such period on record for the state. Mexico experienced a record warm July and August and a warm autumn.

In Canada, 2013 was the thirteenth driest year on record. Nevertheless, torrential downpours overwhelmed Calgary and vast areas of southern Alberta in June, forcing 100 000 people to evacuate their homes and causing close to US\$ 6 billion in damage. The contiguous United States was wetter than average for the year, with some geographical variations. Two states, Michigan and North Dakota, experienced record wet conditions. Alaska observed its third wettest year on record and the wettest in the past 50 years.

A major drought that encompassed large parts of the central United States in 2012 and early 2013 improved across much of the country. By the end of 2013, about 31 per cent of the country was experiencing drought, down from about 61 per cent at the beginning of the year. California had its driest year since records began in 1895; San Francisco received only 16 per cent

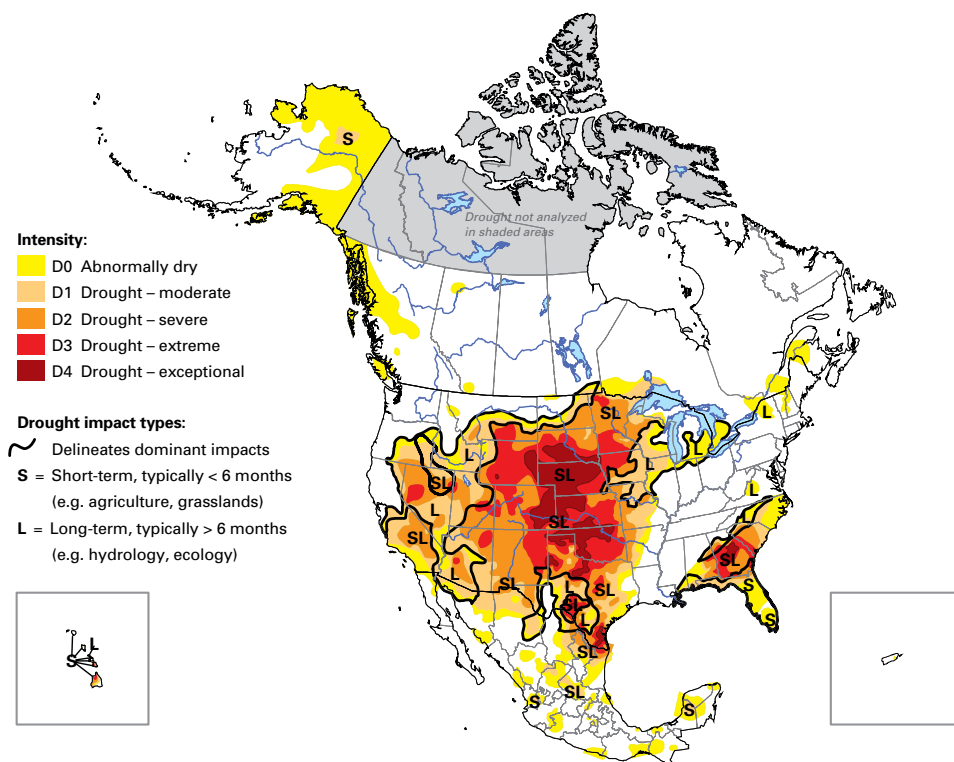


Figure 11. Drought conditions over North America for the beginning of 2013 (Sources: NOAA National Climatic Data Center, in association with the United States Department of Agriculture, the NOAA Climate Prediction Center and the National Drought Mitigation Center, United States; Environment Canada and Agriculture and Agri-Food, Canada; the Comisión Nacional del Agua, and the Servicio Meteorológico Nacional, Mexico)

of its average annual rainfall since local records began in 1947. Very hot conditions, combined with strong winds and drought, contributed to the worst wildfire in Colorado history.

The contiguous United States was hit by several late-season winter storms. In April, Bismarck, North Dakota received 44 cm of snow, setting a new calendar-day record. Duluth, Minnesota and Rapid City, South Dakota each had their snowiest month on record, with 129 cm and 109 cm, respectively. El Reno, Oklahoma, was struck by a particularly powerful tornado: at 4.3 km, it was the widest tornado ever observed in the United States.

In the Caribbean, the Guadeloupe archipelago experienced strong drought conditions between January and March, and the lack of rain damaged sugar cane and banana crops. Martinique received exceptionally heavy rainfall in April.

### SOUTH-WEST PACIFIC

In Australia, 2013 was the warmest year since national records began in 1910, at 1.20°C above average and 0.17°C higher than the previous record in 2005. January was the hottest month ever observed in the country. The summer (December–February) and spring (September–November) were both the hottest on record, and the winter (June–August) was the third warmest. On 7 January, a new national average

daily maximum temperature of 40.30°C was set. The temperature in Moomba, South Australia, reached 49.6°C, the highest recorded in the state since 1960. Hobart recorded its all-time high observed temperature of 41.8°C on 4 January, while the temperature in Sydney reached 45.8°C on 18 January, the hottest since records began. During the same month, a tropical low caused major flooding along much of the east coast of Queensland and northern New South Wales. In Queensland, five people were killed and 8 000 residents were forced to evacuate as floods reached record heights.

New Zealand experienced its warmest winter on record and its third warmest year overall since national records began in 1909. The northern and eastern parts of the country had their driest year on record and suffered drought, while other parts experienced near-record high annual rainfall.

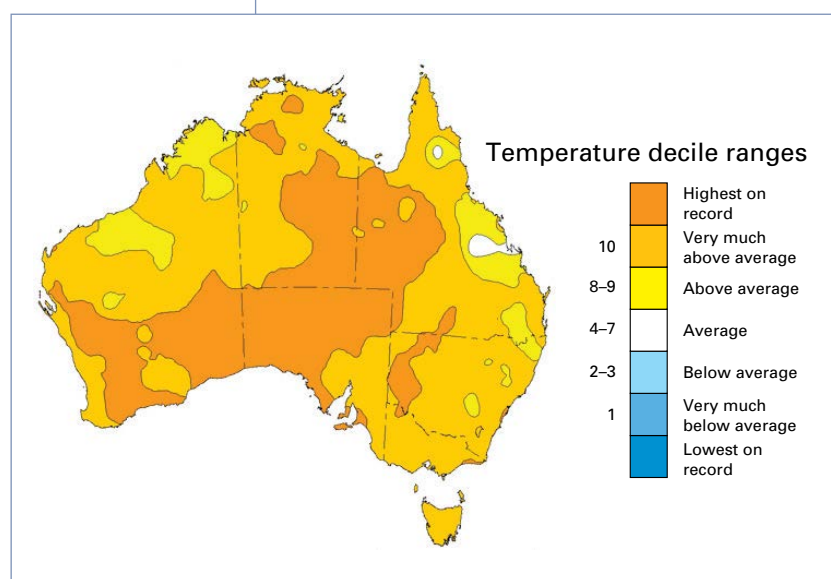
Drier-than-normal weather conditions since late 2012 resulted in severe drought conditions in the northern Marshall Islands. This led to critical shortages of drinking water, damaged food crops and the declaration of a national state of disaster. Abundant rain fell in June over the south of Atuona in the Marquesas Islands of French Polynesia. On 5 June, the region received 66.1 mm of precipitation in one hour. Heavy rains following an extra-tropical depression fell on New Caledonia during 1–3 July. A total of 714 mm of rain fell in a 24-hour period, setting a new record.

### EUROPE AND THE MIDDLE EAST

The year 2013 was the sixth warmest on record across Europe. Many regions were warmer than average at the start of 2013. The north-east of Iceland had its warmest January–February period on record. In Lithuania, February was 3°C warmer than average. However, the Jungfraujoeh in the high mountains of Switzerland saw its coldest winter in the past 40 years.

The north of the European part of the Russian Federation experienced the coldest March in the past half century, as temperatures plunged 8°C–10°C below average in some areas. France, the Netherlands and the United Kingdom all had their coolest springs in decades. In Iceland, a

Figure 12. Annual (1 January–31 December) average temperature deciles map for Australia for the period 1910–2013 (Source: Australian Bureau of Meteorology)





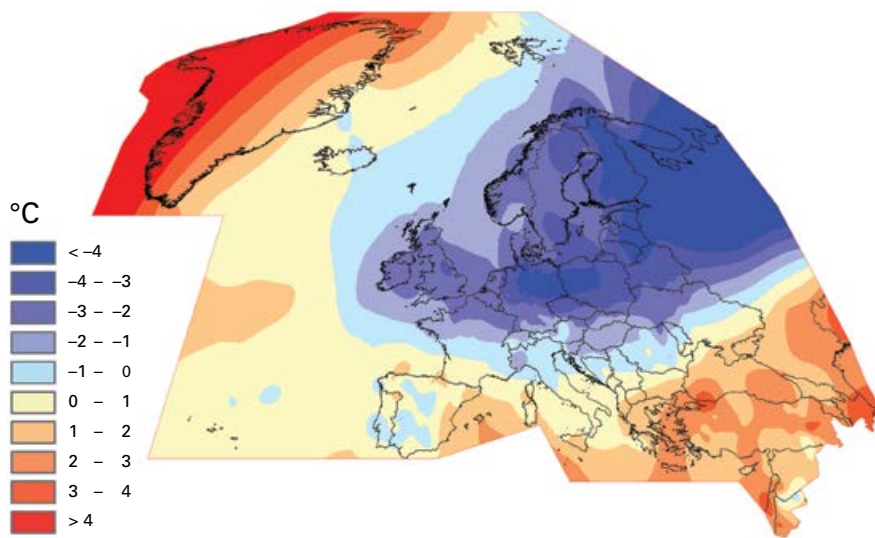


Figure 13. Temperature anomalies over Europe during March 2013 (Source: Deutscher Wetterdienst, Germany)

new minimum record for May was set when the temperature fell to  $-21.7^{\circ}\text{C}$  in the eastern inland. At the same time, the western Greenland coast had its record warmest March, and Norway and Sweden each observed one of their warmest months of May since their national records began.

Summer was very hot for many European countries. Portugal endured one of its worst July heatwaves since 1941. The extended August heatwave in Austria set a new national record high of  $40.5^{\circ}\text{C}$ . On 8 August, many stations in Slovenia observed their highest temperatures on record, with several exceeding  $40^{\circ}\text{C}$ . On the same day in Slovakia, the temperature in Bratislava reached  $39.4^{\circ}\text{C}$ , the highest since observations began in 1850.

The beginning of autumn was also anomalously warm over Europe. Unusual warmth settled over the Russian Federation towards the end of 2013. Following its record warmest November of  $5.3^{\circ}\text{C}$  above the 1961–1990 average, the country observed its record warmest December, at  $4.6^{\circ}\text{C}$  above average. Moscow and Saint Petersburg broke their daily maximum temperature records on 25 December by  $0.4^{\circ}\text{C}$  and  $1.4^{\circ}\text{C}$ , respectively.

Extreme precipitation in the Alpine region and in Austria, Czech Republic, Germany, Poland and Switzerland caused the most intense and extended flooding in the Danube and Elbe river

catchments since at least 1950, as more than 400 mm of rain fell in some localized areas during 29 May–3 June. Austria observed its wettest May–June period since records began in 1858. Some rivers reached historical record heights; in Germany, Passau saw its highest water level since 1501.

During 10–15 December, a rare snowstorm hit parts of the Middle East. In Egypt, snow fell in Cairo for the first time in 112 years. The Syrian Arab Republic, Jordan and Israel also received unprecedented amounts of snow. Cold weather accompanied the storm. On 15 December, the temperature in Shoubak, Jordan, plummeted to  $-16^{\circ}\text{C}$ , the lowest temperature ever recorded in the country.

An extra-tropical cyclone struck the United Kingdom on 28 October, the strongest autumn storm to hit the region since 2002. During 4–7 December, an extra-tropical cyclone moved from west to east across northern Europe; the resulting storm surges, including in the United Kingdom and the Netherlands, were the worst in the past six decades. In Germany, the storm surge reached 4–6 m above mean sea level, but dykes were 8 m tall.

## TROPICAL CYCLONES

Globally, there were 94 storms during 2013 (wind speeds equal to or greater than  $63\text{ km/h}$ ).

The number of storms was higher than in 2012 (84 storms), 2011 (74 storms) and 2010 (67 storms, the lowest number in the modern satellite era). It should be noted that the total number of storms does not necessarily correlate with the number of storms that affect inhabited land areas.

The Atlantic Ocean basin experienced 13 named storms, just above the 1981–2010 average of 12 storms, but below the recent decade of 2001–2010, which saw an average of 15 storms per year. No storms attained major intensity (wind speed of 178 km/h). The intensity and duration of the season's hurricanes were measured as 33 per cent of the average, the lowest value since 1994.

The Eastern North Pacific basin had above-average hurricane activity in 2013. There were a total of 20 storms, 9 of which intensified to hurricane status and 1 of which (*Raymond*) became a major hurricane. Two hurricanes from two separate basins (*Ingrid* in the North Atlantic and *Manuel* in the Eastern North Pacific) struck Mexico nearly simultaneously on 15 September. This unusual event, which had not occurred

since 1958, displaced tens of thousands of residents and damaged some 22 000 homes in Guerrero state.

The Western North Pacific Ocean basin recorded a total of 31 storms, above the 1981–2010 average of 26 and well above the most recent decadal average (2001–2010) of 23, making this the most active season since 2004. Of these storms, 13 strengthened into typhoons. Typhoon *Usagi* (*Odette*) was one of the strongest cyclones globally to have formed in 2013, with 10-minute wind speeds reaching 204 km/h. In November, Typhoon *Haiyan* (named *Yolanda* in the Philippines) became one of the strongest storms on record to ever make landfall anywhere on the globe, with maximum 10-minute wind speeds reaching 230 km/h prior to landfall. *Haiyan* caused significant damage across South-East Asia, and the Philippines bore the brunt of the devastation. Storm surges of 5–6 m were reported in heavily populated low-lying areas of Tacloban and in the islands of Samar and Leyte. Damage caused by immediate surge and following inundation was the worst in the past several decades, with more than 6 200 deaths and



Typhoon *Haiyan* approaching the Philippines on 7 November 2013

NASA

about 14 million people affected, according to reports from the United Nations Office for the Coordination of Humanitarian Affairs. The Philippine National Disaster Risk Reduction and Management Council estimated that total damages exceeded US\$ 850 million in that country alone.

The North Indian Ocean basin recorded a slightly above-average season with five storms compared with the 1981–2010 average of four; three of these storms (*Phailin*, *Lehar* and *Madi*) evolved into very severe cyclonic storms. *Phailin* forced 1.1 million residents in Odisha and Andhra Pradesh states to be evacuated ahead of the storm, one of the largest such evacuations in the history of India.

Ten tropical storms were observed in the South-West Indian Ocean basin during the 2012/2013 tropical cyclone season. This is close to the long-term 1981–2010 average and the 2001–2010 average of nine tropical storms. Seven of these storms reached tropical cyclone status, which is well above the average of four.

The Australian basin recorded a near-average 2012/2013 cyclone season, with 10 tropical storms compared with the 1981–2010 average of 11 and the most recent decadal average of 9. Four of these storms became severe tropical cyclones. The strongest cyclone of the season was *Rusty*, with a financial impact likely exceeding US\$ 100 million.

In the South-West Pacific Ocean basin, the 2012/2013 tropical cyclone season was well below average, with 5 named tropical storms compared with the 1981–2010 average of 12 and the 2001–2010 decadal average of 10. Four of these storms attained severe tropical cyclone status, similar to the 1981–2010 average. Severe Tropical Cyclone *Evan* was the strongest storm in the basin during the season, killing 10 people and causing damages of over US\$ 300 million in Samoa and Fiji alone.

### GREENHOUSE GASES AND OZONE-DEPLETING SUBSTANCES

The WMO Global Atmosphere Watch Programme reports that atmospheric levels of CO<sub>2</sub>, methane (CH<sub>4</sub>) and nitrous oxide (N<sub>2</sub>O) reached new highs in 2012. Data for 2013 have not yet been compiled. Globally averaged levels of CO<sub>2</sub> reached 393.1±0.13 parts per million (ppm), 41 per cent above pre-industrial levels (before 1750). In May 2013, for the first time since observations began, daily average CO<sub>2</sub> levels at several stations outside the Arctic exceeded the symbolic threshold of 400 ppm. (CO<sub>2</sub> levels reach a seasonal maximum in the northern hemisphere spring, before vegetation growth and other processes start to absorb the CO<sub>2</sub>.)

Atmospheric concentrations of CH<sub>4</sub> reached a new high of 1 819±1 parts per billion (ppb) in 2012, or 160 per cent higher than the pre-industrial level. Concentrations of N<sub>2</sub>O reached

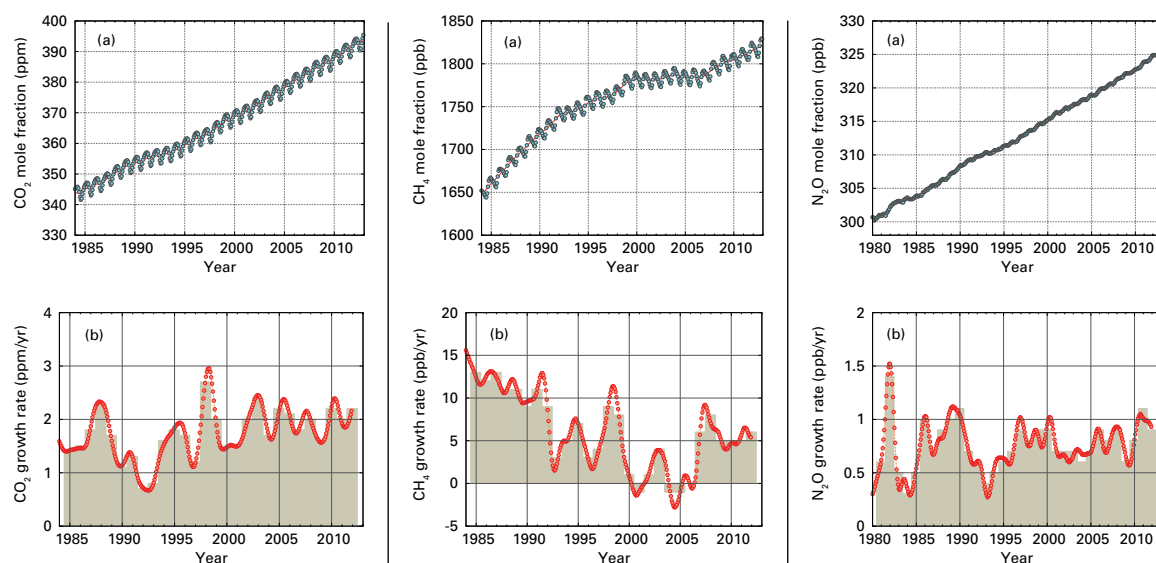


Figure 14. Left: Globally averaged CO<sub>2</sub> mole fraction (a) and its growth rate (b) from 1984 to 2012. Annually averaged growth rate is shown as columns in (b). Centre: Globally averaged CH<sub>4</sub> mole fraction (a) and its growth rate (b) from 1984 to 2012. Annually averaged growth rate is shown as columns in (b). Right: Globally averaged N<sub>2</sub>O mole fraction (a) and its growth rate (b) from 1980 to 2012. Annually averaged growth rate is shown as columns in (b).

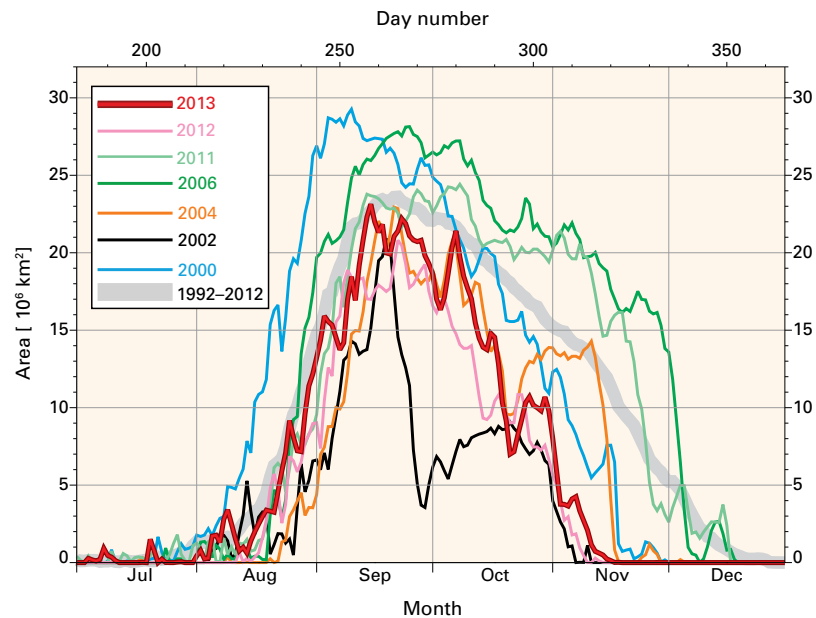
Figure 15. Daily area (million km<sup>2</sup>) of the Antarctic ozone hole for 2013 compared with the two previous ozone holes (2012 and 2011). The plot covers the period from 1 July to 31 December. Also shown for comparison are two years that experienced weak ozone holes (2004 and 2002). The two largest ozone holes on record (in 2000 and 2006) are also shown. The thick light grey line shows the daily ozone hole area averaged over 1992–2012. The plot is produced at WMO and based on data from the Multi Sensor Reanalysis (MSR) of the Royal Netherlands Meteorological Institute until 2008 and on GOME-2 data from the EUMETSAT-operated Metop-A satellite from 2009. More information about the MSR dataset can be found at <http://www.atmos-chem-phys.net/10/11277/2010/acp-10-11277-2010.pdf>.

325.1±0.1 ppb, which is 20 per cent above the pre-industrial level.

As a result, the NOAA Annual Greenhouse Gas Index for 2012 was 1.32, representing a 32 per cent increase in total radiative forcing (relative to 1750) by all long-lived greenhouse gases since 1990. Rising concentrations of greenhouse gases are the main driver of climate change.

While chlorofluorocarbons, halons and other harmful chemicals have been phased out under the Montreal Protocol on Substances

that Deplete the Ozone Layer, these gases can remain in the atmosphere for many years. They deplete the stratospheric ozone layer that protects life on Earth. The resulting Antarctic ozone hole contributes to changes in wind patterns and the regional climate in Antarctica. The Antarctic ozone hole reached a maximum of 23.1 million km<sup>2</sup> on 15 September and 24 million km<sup>2</sup> on 16 September. This is more than the seasonal maxima observed in 2010 and 2012, but somewhat less than the 24.4 million km<sup>2</sup> seasonal maximum reached in 2011.



## MAJOR WEATHER AND CLIMATE EVENTS AROUND THE WORLD IN 2013

- Typhoon *Haiyan (Yolanda)*, one of the strongest storms to ever make landfall, devastated parts of the central Philippines.
- Surface air temperatures over land in the southern hemisphere were very warm, resulting in widespread heatwaves; Australia saw record warmth for the year, Argentina its second warmest year and New Zealand its third warmest.
- Frigid polar air swept across parts of Europe and the south-eastern United States.
- Severe drought gripped Angola, Botswana and Namibia.
- Heavy monsoon rains led to severe floods on the India-Nepal border.
- Abundant rains and flooding impacted north-eastern China and eastern Russian Federation.
- Heavy rains and floods affected Sudan and Somalia.
- Major drought affected southern China.
- North-eastern Brazil experienced its worst drought in the past 50 years.
- The widest tornado ever observed hit El Reno, Oklahoma in the United States.
- Extreme precipitation led to severe floods in the Alps and in Austria, the Czech Republic, Germany, Poland and Switzerland.
- Israel, Jordan and the Syrian Arab Republic were struck by unprecedented snowfall.
- An extra-tropical windstorm affected several countries in western and northern Europe.
- Greenhouse gas concentrations in the atmosphere reached record highs.
- The global oceans reached new record high sea levels.
- The Antarctic sea-ice extent reached a record daily maximum.

# Explaining the summer 2012/2013 and annual 2013 record warmth in Australia

Sophie C. Lewis and David J. Karoly, ARC Centre of Excellence for Climate System Science, University of Melbourne, Australia

## THE IMPORTANCE OF ATTRIBUTION SCIENCE

In 2012, the World Climate Research Programme (WCRP), which is sponsored by WMO, the Intergovernmental Oceanic Commission of the United Nations Educational, Scientific and Cultural Organization and the International Council for Science, identified six grand challenges within the climate science community. The prediction and attribution of extreme events is one of these grand challenges. Extreme climate events that have large impacts on society, both physically and economically, are increasingly requiring prompt and credible scientific explanations.

Today, there is a growing ability within the climate science community to untangle the complexities of understanding the natural and human-induced factors contributing to specific extreme weather and climate events. Recent analyses of various events show that the effects of natural weather and climate fluctuations played a key role in the intensity and evolution of many extreme events. However, for some events, the analyses revealed compelling evidence that human-caused climate change, due to the emission of heat-trapping gases, also contributed. Understanding the influences on such events helps us to better understand how and why extreme events are changing. In addition, calculating how the odds of a particular extreme event have changed provides a way to quantify the influence of climate change on these events.

The Australia summer 2012/2013 area-averaged surface air temperature was the hottest since national records began in 1910. In addition to the summer, temperature records were also broken on daily and monthly timescales. Later in 2013, new national 12-month period temperature records were set in three consecutive months: for the period ending in August, then in September and once again in October. Lastly, a new calendar-year record was set at the end of 2013.

Contributing factors to these record 2013 Australian temperatures, including

human-induced climate change and natural variability associated with El Niño-Southern Oscillation (ENSO), were investigated using a suite of climate model simulations. Using nine state-of-the-art global climate models that participated in the WCRP Coupled Model Intercomparison Project Phase 5, changes in the probability of extreme Australian summer temperatures due to human influences were investigated. These nine models simulate well the observed probability distribution of Australian average summer and 12-month average temperatures since 1910.

The probability of hot Australian summers was calculated for model experiments incorporating human influences (changes in the concentrations of greenhouse gases, aerosols and ozone in the atmosphere) and natural causes (solar radiation changes and emissions from volcanic eruptions), and this was compared with the results from a parallel set of experiments that included only natural causes. The comparison shows that human-induced climate change substantially increased the likelihood of the record-breaking Australian summer of 2013; when human influences were included in model simulations, the probability of very hot summer temperatures across Australia, such as in 2013, increased at least fivefold. These types of extreme Australian summers become even more frequent in simulations of the future under further global warming.

The recent record Australian summer was also notable because it occurred when ENSO conditions were neutral to weak La Niña; these conditions typically produce cooler temperatures across Australia. Prior to 2013, six of the eight hottest Australian summers occurred during El Niño years, but natural ENSO variations are very unlikely to explain the record 2013 Australian heat.

Using the same modelling approach, preliminary analysis of the Australian area-average temperature record for the calendar year 2013 indicates that human-induced causes vastly increased the odds of setting a new

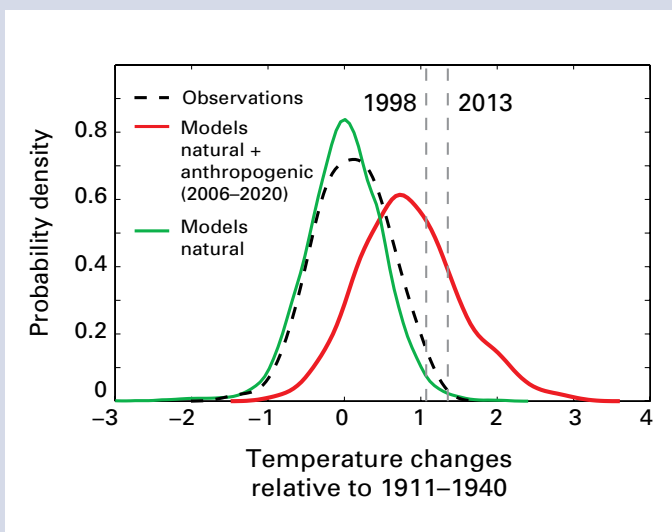
temperature record. In the model experiments, it is virtually impossible to reach such a high temperature due to natural climate variations alone. In simulations with only natural causes considered, none of the 13 000 model years analysed exceed the previous hottest year in Australia, which was observed in 2005. Conversely, in simulations for the period 2006–2020 that include both natural and human-induced causes, such records occur approximately once every 10 years.

In summary, comparing climate model simulations with and without human factors shows that the record hot Australian summer of 2012/2013 was about five times as likely as a result of human-induced influence on climate and that

the record hot calendar year of 2013 would have been virtually impossible without human contributions of heat-trapping gases, illustrating that some extreme events are becoming much more likely due to climate change.

**Attributing Australia’s record warm summer 2012/2013 and record warm calendar year 2013 to human influences** – Sophie C. Lewis and David J. Karoly, ARC Centre of Excellence for Climate System Science, University of Melbourne, Australia. Adapted from: “Anthropogenic contributions to Australia’s record summer temperatures of 2013”, *Geophysical Research Letters*, 40(14):3705–3709 (28 July 2013), available at <http://onlinelibrary.wiley.com/doi/10.1002/grl.50673/abstract>.

Probability density functions for Australian summer temperature anomalies (relative to 1911–1940) for observations (dashed black, all years shown); model simulations considering only natural causes (green, all years shown); and model simulations considering both anthropogenic and natural causes (red, years 2006–2020 shown). Vertical dashed lines show the observed 2013 temperature anomalies for the 2012/2013 Australian summer and the second hottest Australian summer on record (1997/1998).



For more information, please contact:

**World Meteorological Organization**

7 bis, avenue de la Paix – P.O. Box 2300 – CH 1211 Geneva 2 – Switzerland

**Communications and Public Affairs Office**

Tel.: +41 (0) 22 730 83 14/15 – Fax: +41 (0) 22 730 80 27

E-mail: [cpa@wmo.int](mailto:cpa@wmo.int)

[www.wmo.int](http://www.wmo.int)